FULL PAPER *Anatomy*

Comparative study of dermal components and plasma TGF-β1 levels in *Slc39a13/Zip13*-KO mice

Takuya HIROSE[1)], Takayuki OGURA[2)], Keisuke TANAKA[2)], Jun MINAGUCHI[1)] Takeshi YAMAUCHI[1,3)], Toshiyuki FUKADA[4,5,6)], Yoh-ichi KOYAMA[2)] and Kazushige TAKEHANA[1)]*

[1)]*Department of Veterinary Microanatomy, School of Veterinary Medicine, Rakuno Gakuen University, Ebetsu, Hokkaido 069–8501, Japan*
[2)]*Nippi Research Institute of Biomatrix and Protein Engineering Project, Toride, Ibaraki 302–0017, Japan*
[3)]*The Maple Foundation, Chuou-ku, Tokyo 103–0014, Japan*
[4)]*RIKEN Center for Integrative Medical Sciences, Yokohama, Kanagawa 230–0045, Japan*
[5)]*Division of Pathology, Department of Oral Diagnostic Sciences, Showa University School of Dentistry, Shinagawa, Tokyo 142–8555, Japan*
[6)]*Molecular and Cellular Physiology, Faculty of Pharmaceutical Sciences, Tokushima Bunri University, Tokushima 770–8055, Japan*

(Received 8 January 2015/Accepted 22 May 2015/Published online in J-STAGE 5 June 2015)

ABSTRACT. Ehlers-Danlos syndrome (EDS) is a group of disorders caused by abnormalities that are identified in the extracellular matrix. Transforming growth factor-β1 (TGF-β1) plays a crucial role in formation of the extracellular matrix. It has been reported that the loss of function of zinc transporter ZRT/IRT-like protein 13 (ZIP13) causes the spondylocheiro dysplastic form of EDS (SCD-EDS: OMIM 612350), in which dysregulation of the TGF-β1 signaling pathway is observed, although the relationship between the dermis abnormalities and peripheral TGF-β1 level has been unclear. We investigated the characteristics of the dermis of the *Zip13*-knockout (KO) mouse, an animal model for SCD-EDS. Both the ratio of dermatan sulfate (DS) in glycosaminoglycan (GAG) components and the amount of collagen were decreased, and there were very few collagen fibrils with diameters of more than 150 nm in *Zip13*-KO mice dermis. We also found that the TGF-β1 level was significantly higher in *Zip13*-KO mice serum. These results suggest that collagen synthesis and collagen fibril fusion might be impaired in *Zip13*-KO mice and that the possible decrease of decorin level by reduction of the DS ratio probably caused an increase of free TGF-β1 in *Zip13*-KO mice. In conclusion, skin fragility due to defective *ZIP13* protein may be attributable to impaired extracellular matrix synthesis accompanied by abnormal peripheral TGF-β homeostasis.
KEY WORDS: dermatan sulfate, plasma TGF-β1 level, *Zip13*-KO mouse

doi: 10.1292/jvms.15-0015; *J. Vet. Med. Sci.* 77(11): 1385–1389, 2015

Ehlers-Danlos syndrome (EDS) is an inherited disorder of connective tissue characterized by skin hyperelasticity, skin fragility (easy rupture), articular hypermobility and vascular fragility [7]. Types of EDS are classified according to its causes, including molecular abnormality of collagen, defective fibronectin, lack of type I procollagen N-proteinase activity and lack of dermatan sulfate caused by aplasia of the core protein of decorin [5, 7, 19]. Compared with normal skin, the major morphological and biochemical characteristics of EDS skin are higher levels of matrix substrates, thicker collagen fibers, less density of fiber bundles in the reticular layer and less uniformity of fiber orientations. It was reported that the thickness of the reticular layer in EDS patients was only about one third of that in normal subjects [10]. Such characteristics are responsible for the large polydispersity index, which indicates the degree of distribution of fine collagen fibers [6].

Transforming growth factor-β1 (TGF-β1) is the primary member of the TGF-β family [17]. TGF-β1 functions to increase components of the extracellular matrix not only by promoting the production of collagens and proteoglycans but also by inhibiting the production of various proteases [13]. TGF-β1 is inactive when combined with decorin, a proteoglycan in the extracellular matrix, and it becomes active only when it separates from decorin [3]. TGF-β1 binds to its receptor component, and SMAD transcription factors are subsequently phosphorylated by the activated receptors. SMAD proteins then move into the nucleus and promote transcription of target genes leading to the synthesis and accumulation of the extracellular matrix [14, 16]. Marfan syndrome is one of the genetic diseases in which systemic fragility of connective tissues occurs as a result of genetic mutations, including mutations in fibrillin-1 and TGF-β receptor 2 genes [11, 18].

Slc39a13/ZIP13 is a member of the Slc39/ZIP zinc transporter family [8] localized mainly in the Golgi apparatus of osteoblasts, chondrocytes, odontoblasts and fibroblasts. It is involved in the transport of zinc from the Golgi apparatus to the cytoplasm and controls the nuclear shift of SMAD proteins in TGF-β1 and bone morphogenetic protein (BMP) signaling pathways [1, 2, 9, 17]. Loss of ZIP13 function causes perturbations of these pathways, and thus, there is little synthesis of the extracellular matrix. This assumption is strongly supported by the results of a study on a defect

*CORRESPONDENCE TO: TAKEHANA, K., Department of Veterinary Microanatomy, School of Veterinary Medicine, Rakuno Gakuen University, Ebetsu, Hokkaido 069-8501, Japan.
e-mail: takechan@rakuno.ac.jp

of a gene that regulates dematan sulfate proteoglycan in cattle with a variant form of EDS in which glycosaminoglycan (GAG) consisted almost solely of hyaluronic acid [19]. *Zip13*-knockout (KO) mice, an animal model for the spondylocheiro dysplasic form of EDS (SCD-EDS: OMIM 612350), show skeletal and connective tissue disorder [9].

Since the relationship between EDS pathogenesis and peripheral TGF-β1 levels has not yet been clarified, *Zip*13-KO mice were used in this study to clarify the relationship between plasma TGF-β1 levels and clinical conditions of SCD-EDS.

MATERIALS AND METHODS

Animals and experimental design: Mice were weaned at 4 weeks of age, and 3 mice were used for each genotype group: wild-type (WT) group and *Zip13*-KO (KO) group. All animals were sacrificed at 8 weeks of age for the experiments. Skin samples were taken from the pre-scapular and dorsal regions used for generally ultrastructural investigation of skin [15] immediately after euthanasia, and the samples were processed for light and electron microscopic investigation or were frozen and prepared for GAG analysis.

The animal experiments were approved by the Ethics Committee of Rakuno Gakuen University.

Morphological analysis: Light microscopy.

Samples were fixed in Bouin's fixative for 24 hr at room temperature. After dehydration through ethanol and xylol series, samples were embedded in paraffin. Eight-μm-thick sections were cut in the epidermal-dermal direction and then dewaxed and stained with hematoxylin and eosin. Dermal thickness was measured at 5 points from 8 areas in each sample (120 points/24 areas/3 mice/group), and the number of cells per 0.01 mm^2 was counted.

Transmission electron microscopy (TEM).

Samples (0.5 × 0.5 × 0.5 mm) were fixed in 3.0% glutaraldehyde in 0.1 M phosphate buffer (pH 7.4) for 2 hr at room temperature. The samples were then post-fixed in 1.0% osmium tetroxide in 0.1 M phosphate buffer for 1 hr at room temperature. Thereafter, samples were washed with distilled water, dehydrated in graded ethanol series and embedded in Quetol 812 (Nissin EM, Tokyo, Japan). Sections of approximately 60 nm in thickness were cut with a Reichert Supernova system (Leica, Vienna, Austria) equipped with a diamond knife. Sections were mounted on a copper grid and consecutively stained with 0.2% tannic acid + 10% ethanol in water for 15 min, 1.0% uranyl acetate for 5 min and 1.0% lead citrate for 10 sec. A TEM (JEM-1220; JEOL, Tokyo, Japan) at an accelerating voltage of 80 kV was used for the investigation. Five hundred fibrils randomly selected from bottom of dermal layer in photographs of each skin sample were measured by Image J, and the average value was obtained.

Biochemical analysis: Analysis of amino acid.

After the addition of 6N HCl, skin samples were punched using a trephine with a diameter of 5 mm and treated in a heat block at 110°C for 24 hr. The solvent was evaporated in Evaporator. The remaining amino acid was dissolved in 0.02 M HCl. The solution obtained from the filtration was analyzed for amino acid contents. The amount of collagen per unit area was calculated from the amount of hydroxyproline.

Analysis of GAG.

Frozen samples were cut into small blocks on ice. After dehydration and degreasing by stirring in acetone 3 times for 30 min each time at room temperature and then in diethyl ether 3 times for 30 min each time at room temperature, dry weight of the samples was determined. Removal of GAG from proteoglycan core proteins was performed by stirring samples in 20 volumes of 0.5 N NaOH at 4°C for 15 hr. Neutralization was performed in 1 N HCl with a similar condition. Proteins in the mixture were denatured by heating at 100°C for 10 min. The pH of the mixture was adjusted to 8.0 with 1 M Tris-HCl buffer (pH 7.8), and the mixture was digested with 1 mg/m*l* pronase (actinase E; Seikagaku Kougyo, Tokyo, Japan) at 50°C for 24 hr. Trichloroacetic acid was then added to a final concentration of 10%. After incubating for 1 hr, the mixture was centrifuged at 1,600 × *g* for 15 min in order to remove the precipitated proteins, and the supernatant was dialyzed against distilled water at 4°C for 3 days. The dialyzed sample was freeze-dried and subjected to two-dimensional electrophoresis on a cellulose acetate membrane. GAG was stained with a solution containing 0.1% alcian blue 8GX (Merck, Darmstadt, Germany) and 0.1% acetic acid. GAG content was quantified by an assay for hexosamine. Hyaluronic acid, dermatan sulfate, heparin and chondroitin-6-sulphate (Nacalai Tesque, Kyoto, Japan) were used as GAG standards.

Plasma concentration of TGF-β1.

Fresh blood samples were immediately placed in ice for 10–60 min before being centrifuged in a refrigerated (4°C) centrifuge at 1,000 × *g* for 30 min for collection of plasma. The plasma samples were stored at −80°C. A TGF-β1 assay kit (Quantikine Mouse/Rat/Porcine/Canine; R & D Systems, Minneapolis, MN, U.S.A.) was used for the measurement.

Statistical analysis.

Student's *t*-test was used to compare differences among the means of thickness of the dermis, density of cells, amount of collagen and ratio of hydroxyproline at a significant level of P=0.05. Differences in median diameters of collagen fibrils and plasma concentration of TGF-β1 between groups were tested by the Wilcoxon rank sum test at P<0.05.

RESULTS

Morphological analysis: *Light microscopy*: The dermal layer consists of cells and cellular matrix. The major matrix component of the dermal layer is collagen fibrils. Thickness of the dermal layer was measurable. The thickness in the WT group was 231.4 ± 22.1 μm, while that in the KO group was 162.2 ± 22.5 μm (Fig. 1). There was a significant difference between the thicknesses in the 2 groups (P<0.05). Densities of the cellular population in the WT group (24.6 ± 1.5 cells/0.01 mm^2) and KO group (31.0 ± 3.6 cells/0.01 mm^2)

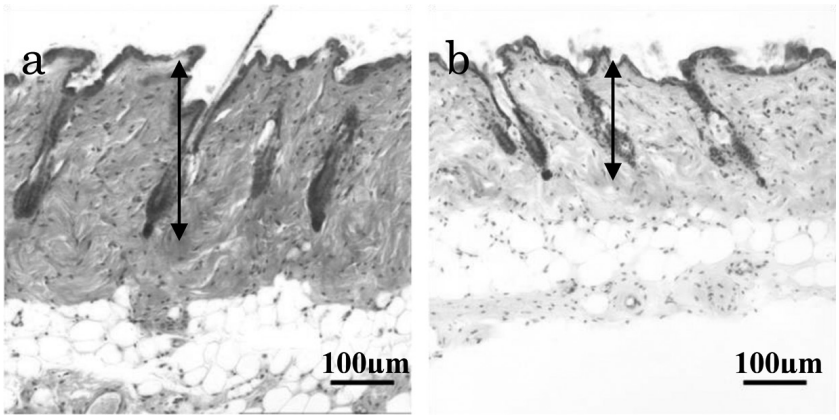

Fig. 1. Light microscopic observation of the H&E-stained dermal layer from WT (a) and KO (b) mice.

Table 1. Morphometric and biochemical analyses of dermal layer and levels of TGF-β1 in plasma from WT and KO mice

Analysis	WT	KO
Thickness of dermis (μm)	231.4 ± 22.1	162.2 ± 22.5*
Density of cells (cells/0.01 mm^2)	24.6 ± 1.5	31.0 ± 3.6*
Median diameter of collagen fibrils (nm)	89.4	81.4
Amount of collagen (μg/mm^2)	72.3 ± 8.8	22.2 ± 2.3*
Ratio of hydroxyproline (residues/1,000 total residues)	95.7 ± 0.9	84.0 ± 2.5*
Ratio of GAG components		
HA (%)	55.5	63.2
DS (%)	44.5	36.8
Plasma concentration of TGF-β1 (*n*g/m*l*)	1.45 ± 0.42	2.74 ± 1.35*

Mean ± SD, *Significantly different (P<0.05).

were significantly different (Table 1).

Transmission electron microscopy.

The diameters of collagen fibrils in the 2 groups were clearly different (Fig. 2). The diameter range of collagen fibrils in the WT group was from 20 to 320 nm with a median of 89.4 nm. There was no collagen fibril with a diameter larger than 200 nm in the KO group (Fig. 2). The fibril diameters in the KO group were limited to 20–200 nm with a median of 81.4 nm (Table 1).

Biochemical analysis: *Analysis of amino acid*: The amount of collagen in the WT group was 72.3 ± 8.8 μg/mm^2, and that in the KO group was 22.2 ± 2.3 μg/mm^2. The ratio of hydroxyproline (residues/1,000 total residues) in the WT group was 95.7 ± 0.9, and that in the KO group was 84.0 ± 2.5 (Table 1).

Analysis of GAG.

In the WT group, the HA ratio was 55.5%, and the DS ratio was 44.5%. In the KO group, HA was 63.2%, and DS was 36.8% (Table 1).

Plasma concentration of TGF-β1.

The plasma concentration of TGF-β1 in the WT group was 1.45 ± 0.42 *n*g/m*l*, and that in the KO group was 2.74 ± 1.35 *n*g/m*l* (Table 1).

DISCUSSION

Zip13-KO mice have been reported to have the following characteristics: zinc concentration in fibroblastic cells lacking ZIP13 is increased in Golgi apparatus and decreased in the nucleus, nuclear transport of SMAD proteins is impaired, and expression level of type I collagen is decreased [9] (Fig. 3). In this study, we clarified the biochemical and histological characteristics of amino acid that constitutes collagen and the composition of the dermal layer of *Zip13*-KO mice.

The histological dermal layer in the KO group was found to be thinner than that in the WT group. In electron microscopic investigation, the dermal layer of 20-week-old mouse shows collagen fibrils over 200-nm in diameter [4]. The ratio of collagen fibrils with diameters of more than 150 nm in the KO group was small. The diminished amount of mature collagen in *Zip13*-KO mice was likely due to the impaired nuclear transport of SMAD proteins in fibroblast lacking [9], suggesting that possible suppression of collagen assembly could occur by decreased signaling of TGF-β in the KO group.

TGF-β1 has multiple functions affecting pleiotropic phenomena, exerting inhibitory effects on cell proliferation for example [12]. The larger number of cells per unit area in the

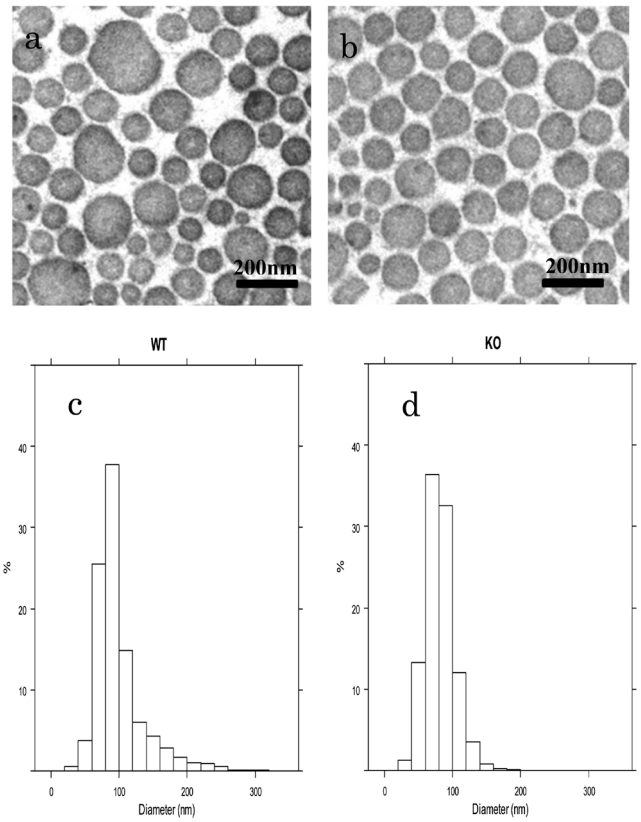

Fig. 2. Transmission electron microscopic observation of collagen fibrils from WT (a) and KO (b) mice. It was clearly seen that collagen fibrils with diameters larger than 200 nm existed only in WT mice. Histogram of diameters of collagen fibrils from WT (c) and KO (d) mice. The diameters of fibrils from WT mice were distributed from 20 to 320 nm, while those of fibrils from KO mice were restricted to 20–200 nm.

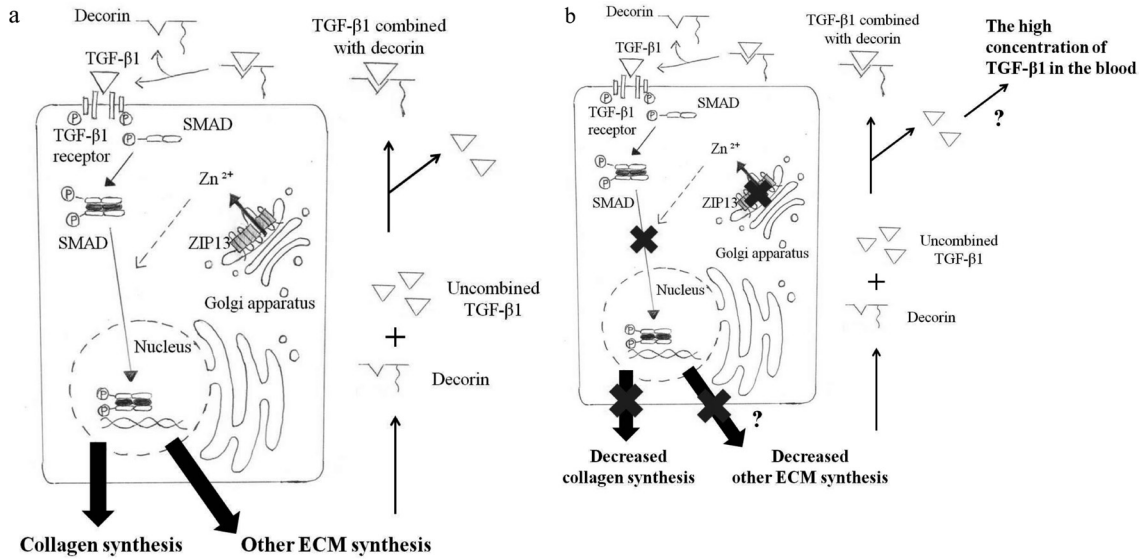

Fig. 3. Outline of relationship between TGF-β1 and collagen synthesis. (a) In normal fibroblast, TGF-β1 binds to its receptor component, and SMAD transcription factors are subsequently phosphorylated by the activated receptors. SMAD proteins then move into the nucleus and promote transcription of target genes leading to the synthesis of collagen. (b) *Zip13*-KO fibroblasts show decreased collagen synthesis most likely due to impaired nuclear transport of SMAD proteins, although *Zip13*-KO mice exhibit higher TGF-β1 levels by unknown mechanisms.

KO group than in the WT group suggested a smaller effect of TGF-β1 in the KO group.

The diameter of collagen fibrils in the KO group was found to be smaller than that in the WT group. Large collagen fibrils are formed by fibril fusion [20]. Fusion of collagen fibrils is probably regulated by decorin, a substance that is known to regulate collagen fibril diameter [20]. Decorin, which carries dermatan sulfate (DS) as a GAG chain, expresses its inhibitory effects through combining with TGF-β1 and sending negative feedback to TGF-β1 [1]. The amount of decorin can be indirectly indicated by the proportion of DS in the GAG chain. Thus, decrease of decorin in the KO group was indicated by a decrease in its proportion of DS compared with that in the WT group. The higher concentration of TGF-β1 in the blood indicated lower negative feedback against TGF-β1 caused by the decrease of decorin.

In conclusion, lack of ZIP13 in fibroblasts resulted in alteration of the composition of the extracellular matrix and decrease in the amount of collagen and diameter of collagen fibrils. Decrease of decorin in the extracellular matrix, which normally increases the uncombined TGF-β1 level in blood, is thought to be the cause of these imbalances leading to skin fragility. Results of further investigations on culture of fibroblasts from *Zip13*-KO mice will contribute to an understanding of the relationship between plasma TGF-β1 and collagen fibrils.

ACKNOWLEDGMENTS. We wish to thank Dr. Hideyuki Asaoka for technical support in measurement of TGF-β1. This work was partially supported by Kaede-kai.

REFERENCES

1. Bin, B. H., Fukada, T., Hosaka, T., Yamasaki, S., Ohashi, W., Hojyo, S., Miyai, T., Nishida, K., Yokoyama, S. and Hirano, T. 2011. Biochemical characterization of human zip13 protein: A homo-dimerizd zinc transporter involved in the spondylocheiro dysplastic ehlers-danlos syndrome. *J. Biol. Chem.* **286**: 40255–40265. [Medline] [CrossRef]
2. Bin, B. H., Hojyo, S., Hosaka, T., Bhin, J., Kano, H., Miyai, T., Ikeda, M., Kimura-Someya, T., Shirouzu, M., Cho, E. G., Fukue, K., Kambe, T., Ohashi, W., Kim, K. H., Seo, J., Choi, D. H., Nam, Y. J., Hwang, D., Fukunaka, A., Fujitani, Y., Yokoyama, S., Superti-Furga, A., Ikegawa, S., Lee, T. R. and Fukada, T. 2014. Molecular pathogenesis of spondylocheirodysplastic ehlers-danlos syndrome caused by mutant zip13 proteins. *EMBO Mol. Med.* **6**: 1028–1042. [Medline] [CrossRef]
3. Border, W. A., Noble, N. A., Yamamoto, T., Harper, J. R., Yamaguchi, Y., Pierschbacher, M. D. and Ruoslahti, E. 1992. Natural inhibitor of transforming growth factor-β protects against scarring in experimental kidney disease. *Nature* **360**: 361–364. [Medline] [CrossRef]
4. Bradshaw, A. D., Puolakkainen, P., Dasgupta, J., Davidson, M. J., Wight, N. T. and Sage, E. H. 2003. SPARC-Null Mice Display Abnormalities in the Dermis Characterized by Decreased Collagen Fibril Diameter and Reduced Tensile Strength. 2003. *J. Invest. Dermatol.* **120**: 949–955. [Medline] [CrossRef]
5. Colige, A., Sieron, A. L., Li, S., Schwarze, U., Petty, E., Wertelecki, W., Wilcox, W., Krakow, D., Cohn, D. H., Reardon, W., Byers, P. H., Lapiere, C. M., Prockop, D. J. and Nusgens, B. V. 1999. Human ehlers-danlos syndrome type VII C and bovine dermatosparaxis are caused by mutations in the procollagen I N-proteinase *Gene*. *Am. J. Hum. Genet.* **65**: 308–317. [Medline] [CrossRef]
6. Craig, A. S. and Parry, D. A. D. 1981. Collagen fibrils of the vertebrate corneal stroma. *J. Ultrastruct. Res.* **74**: 232–239. [Medline] [CrossRef]
7. Deren-Wagemann, I., Kuliszkiewicz-Janus, M. and Schiller, J. 2010. Ehlers-danlos syndrome. *Adv. Clin. Exp. Med* **19**: 537–542.
8. Fukada, T. and Kambe, T. 2011. Molecular and genetic features of zinc transporters in physiology and pathogenesis. *Metallomics* **3**: 662–674. [Medline] [CrossRef]
9. Fukada, T., Civic, N., Furuichi, T., Shimoda, S., Mishima, K., Higashiyama, H., Idaira, Y., Asada, Y., Kitamura, H., Yamasaki, S., Hojyo, S., Nakayama, M., Ohara, O., Koseki, H., Dos Santos, H. G., Bonafe, L., Ha-Vinh, R., Zankl, A., Unger, S., Kraenzlin, M. E., Beckmann, J. S., Saito, I., Rivolta, C., Ikegawa, S., Superti-Furga, A. and Hirano, T. 2008. The zinc transporter SLC39A13/ZIP13 is required for connective tissue development; its involvement in BMP/TGF-beta signaling pathways. *PLoS ONE* **3**: e3642. [Medline] [CrossRef]
10. Hausser, I. and Anton-Lamprecht, I. 1994. Differential ultrastructural aberrations of collagen fibrils in Ehler-Danlos syndrome types I-IV as a means of diagnostics and classification. *Hum. Genet.* **93**: 394–407. [Medline] [CrossRef]
11. Loeys, B. L., Mortier, G. and Dietz, H. C. 2013. Bone lessons from marfan syndrome and related disorders: fibrillin, TGF-β and BMP at the balance of too long and too short. *Pediatr. Endocrinol. Rev.* **10**: 417–423. [Medline]
12. Lyons, R. M. and Harold, L. M. 1990. Transforming growth factors and the regulation of cell proliferation. *Eur. J. Biochem.* **187**: 467–473. [Medline] [CrossRef]
13. Ma, C. and Nasser, C. 1999. Regulation of matrix metalloproteinases (MMps) and their tissue inhibitors in human myometrial smooth muscle cells by TGF-β1. *Mol. Hum. Reprod.* **5**: 950–954. [Medline] [CrossRef]
14. Massagué, J. and Roger, R. G. 2006. The logic of TGFβ signaling. *FEBS Lett.* **580**: 2811–2820. [Medline] [CrossRef]
15. Matsuda, N., Koyama, Y., Hosaka, Y., Ueda, H., Watanabe, T., Araya, T., Irie, S. and Kazushige, T. 2006. Effects of Collagen Peptide on Collagen Fibrils and Glycosaminoglycans in the Dermis. *J. Nutr. Sci. Vitaminol. (Tokyo)* **52**: 211–215. [Medline] [CrossRef]
16. Miyazono, K., Dijke, T. P. and Heldin, C. H. 2000. TGF-β signaling by smad proteins. *Adv. Immunol.* **75**: 115–157. [Medline]
17. Munemasa, T., Idaira, Y., Fukada, T., Shimoda, S. and Asada, Y. 2014. Histological analysis of dentinogesis imperfecta in Slc39a13/Zip13 knockout mice. *J. Hard Tissue Biol.* **23**: 163–168. [CrossRef]
18. Neptune, E. R., Frischmeyer, P. A., Arking, D. E., Myers, L., Bunton, T. E., Gayraud, B., Ramirez, F., Sakai, L. Y. and Dietz, H. C. 2003. Dysregulation of TGF-β activation contributes to pathogenesis in marfan syndrome. *Nat. Genet.* **33**: 407–411. [Medline] [CrossRef]
19. Tajima, M., Miyake, S., Takehana, K., Kobayashi, A., Yamato, O. and Maede, Y. 1999. Gene defect of dermatan sulfate proteoglycan of cattle affected with a variant form of ehlers-danlos syndrome. *J. Vet. Intern. Med.* **13**: 202–205. [Medline] [CrossRef]
20. Watanabe, T., Hosaka, Y., Yamamoto, E., Ueda, H., Sugawara, K., Takahashi, H. and Takehana, K. 2005. Control of the collagen fibril diameter in the equine superficial digital flexor tendon in horses by decorin. *J. Vet. Med. Sci.* **67**: 855–860. [Medline] [CrossRef]